



Molecular Crystals and Liquid Crystals

Publication details, including instructions for authors and subscription information:

<http://www.tandfonline.com/loi/gmcl20>

Chiral Smectics: Molecular Design and Superstructures

Isa Nishiyama^a, Jun Yamamoto^a, John W. Goodby^b
& Hiroshi Yokoyama^{a c}

^a Yokoyama Nano-structured Liquid Crystal Project,
JST, Tokodai, Japan

^b Department of Chemistry, University of York, York,
U.K.

^c Nanotechnology Research Institute, AIST, Tsukuba,
Japan

Version of record first published: 31 Jan 2007

To cite this article: Isa Nishiyama, Jun Yamamoto, John W. Goodby & Hiroshi Yokoyama (2005): Chiral Smectics: Molecular Design and Superstructures, *Molecular Crystals and Liquid Crystals*, 443:1, 25-41

To link to this article: <http://dx.doi.org/10.1080/15421400500236485>

PLEASE SCROLL DOWN FOR ARTICLE

Full terms and conditions of use: <http://www.tandfonline.com/page/terms-and-conditions>

This article may be used for research, teaching, and private study purposes. Any substantial or systematic reproduction, redistribution, reselling, loan, sub-licensing, systematic supply, or distribution in any form to anyone is expressly forbidden.

The publisher does not give any warranty express or implied or make any representation that the contents will be complete or accurate or up to

date. The accuracy of any instructions, formulae, and drug doses should be independently verified with primary sources. The publisher shall not be liable for any loss, actions, claims, proceedings, demand, or costs or damages whatsoever or howsoever caused arising directly or indirectly in connection with or arising out of the use of this material.

Chiral Smectics: Molecular Design and Superstructures

Isa Nishiyama*

Jun Yamamoto

Yokoyama Nano-structured Liquid Crystal Project, JST, Tokodai, Japan

John W. Goodby

Department of Chemistry, University of York, York, U.K.

Hiroshi Yokoyama

Yokoyama Nano-structured Liquid Crystal Project, JST, Tokodai, Japan
and Nanotechnology Research Institute, AIST, Tsukuba, Japan

Molecular design producing a strong chiral effect has been proposed and dichiral twin and monomeric materials have been prepared systematically based on this concept. A variety of superstructures are generated in the chiral smectic phases, including ferroelectric and antiferroelectric phases, a twist grain boundary phase and the variants, such as smectic blue and smectic Q phases, and mysterious isotropic phases exhibiting an anomalous electric-field induced phase transition.

Keywords: chirality; liquid crystal; smectic; TGB; twin

1. INTRODUCTION

Introduction of the chirality has a fascinating effect on producing various kinds of superstructures in liquid-crystalline systems (Fig. 1).

In particular, introduction of chirality in smectic liquid-crystalline systems sometimes produces a variety of frustrated phases, such as twist grain boundary (TGB) [1], smectic blue [2], and smectic Q [3] phases. Not only a family of the TGB phases, but also an interesting example of the effect of chirality can be seen in some dichiral mesogens [4], where the chirality was found to play a dominant role in the appearance of the cubic superstructure [5]. Location of the chiral

Address correspondence to Isa Nishiyama, Yokoyama Nano-structured Liquid Crystal Project, JST, ERATO, TRC 5-9-9, Tokodai, Tsukuba 300-2635, Japan. E-mail: isanishi@db3.so-net.ne.jp

*Present address: Dainippon Ink and Chemicals, Incorporated, Central Research Laboratories, 631 Sakado, Sakura, Chiba 285-8668, Japan.

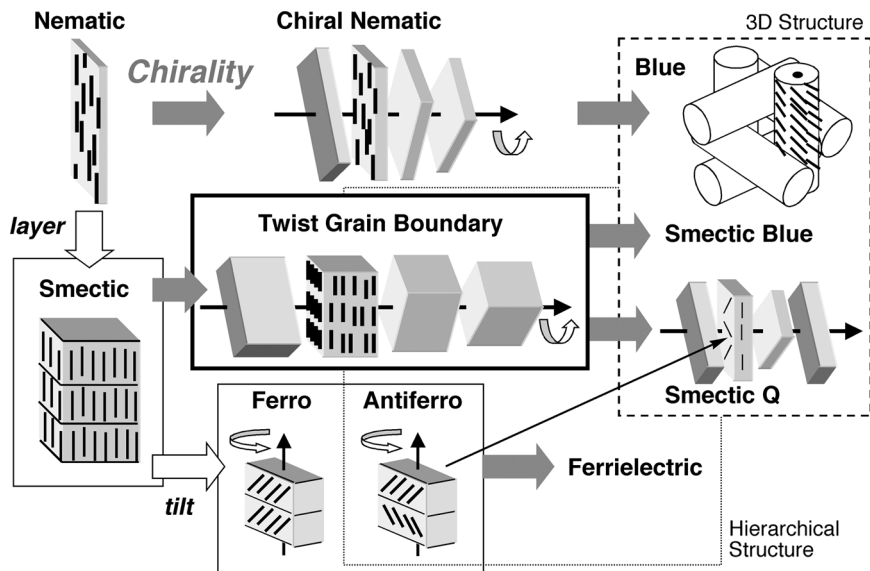


FIGURE 1 Liquid-crystalline superstructures produced by chirality.

moieties in the over-all molecular structure seems to have a significant effect on the appearance of these chirality-induced frustrated superstructures. For example, compounds showing the SmQ phase possess identical chiral moieties at both sides of the rigid core [3], and the dichiral mesogen showing a chirality-induced cubic phase also possesses two chiral moieties with different structures at both peripheral ends of the rigid core part [4]. In this paper, a variety of chirality-induced phenomena observed in newly designed dichiral molecules are reviewed. In particular, the effect of introducing a non-symmetric structure and the anomalous property observed in the isotropic phase of the dichiral compounds are reported in detail.

2. EXPERIMENTAL

Final compounds were prepared by the esterification using a DCC/DMAP method. Optically active phenolic intermediates were prepared using a Mitsunobu coupling. In the synthesis, the chiral alcohols, (S)-2-octanol (Azmax. Co. Ltd., 99% ee) and (R)-2-octanol (Azmax. Co. Ltd., 99% ee), were used without further purification. The structures of the materials were elucidated by elemental analyses, IR spectroscopy, ^1H NMR spectrometry, and MS spectrometry. The analyses of the structures of the products were found to be consistent

with the predicted structures. Examples of the preparation of the final compounds are shown below.

Preparation of 4'-((R)-1-methylheptyloxycarbonyl)-1,1'-biphenyl-4-yl 6'''-[5-[[4''-((R)-1-methylheptyloxycarbonyl)-1'',1'''-biphenyl-4'''-yl]oxycarbonyl]-pentyloxy]naphtyl-2'''-carboxylate (III)

6-(5-Carboxypentyloxy)naphtyl-2-carboxylic acid (0.60 g, 2.0 mmol), (R)-1-methylheptyl 4-hydroxybiphenyl-4'-carboxylate (1.30 g, 4.0 mmol), and DMAP (0.05 g, 0.4 mmol) were added to dry dichloromethane (10 ml). DCC (1.23 g, 6.0 mmol) was then added and the resulting mixture was stirred at room temperature for one day. Precipitated materials were removed by filtration. After removal of the solvent by evaporation under reduced pressure, the product was purified by column chromatography over silica gel (70–230 mesh, Sigma-Aldrich Co.) using a mixture of dichloromethane/hexane (5:2) as the eluent, and the resulting product was recrystallised from an ethanol/ethylacetate (3:1) mixture (40 ml), to give a colourless solid. Yield = 0.86 g, (47%). δ H (300 MHz, CDCl₃, TMS); 8.73 (m, 1H, Ar-H), 8.19–8.09 (m, 5H, Ar-H), 7.90 (m, 1H, Ar-H), 7.81 (m, 1H, Ar-H), 7.71–7.61 (m, 8H, Ar-H), 7.38–7.17 (m, 6H, Ar-H), 5.19 (m, 2H, -C*H(CH₃)-), 4.18 (t, 2H, -CH₂O-, 3J = 6.2 Hz), 2.67 (t, 2H, -CH₂OCO-, 3J = 7.3 Hz), 2.00–1.29 (m, 32H, aliphatic-H), 0.89 (two overlapping triplets, 6H, -CH₂-CH₃). ν /cm⁻¹ (KBr); 2930, 2859 (C-H str.), 1732, 1717 (C=O str.), 1628, 1609 (C-C str.). m/z ; 918 (M⁺), 459. HPLC purity; Normal phase: 100%, Reverse Phase: 99.6%.

Preparation of 4'-((R)-1-methylheptyloxycarbonyl)-1,1'-biphenyl-4-yl 4'''-[5-[[4''-((R)-1-methylheptyloxycarbonyl)-1'',1'''-biphenyl-4'''-yl]oxycarbonyl]pentyloxy]-1''' ,1'''''-biphenyl-4'''-carboxylate (IV)

4'-(5-Carboxypentyloxy)biphenyl-4-carboxylic acid (0.65 g, 2.0 mmol), (R)-1-methylheptyl 4-hydroxybiphenyl-4'-carboxylate (1.30 g, 4.0 mmol), and DMAP (0.05 g, 0.4 mmol) were added to dry dichloromethane (10 ml). DCC (1.23 g, 6.0 mmol) was then added and the resulting mixture was stirred at room temperature for one day. Precipitated materials were removed by filtration. After removal of the solvent by evaporation under reduced pressure, the product was purified by column chromatography over silica gel (70–230 mesh, Sigma-Aldrich Co.) using a mixture of dichloromethane/hexane (10:3) as the

eluent, and the resulting product was recrystallised from a mixture of ethanol/ethylacetate (50 ml:42 ml), to give a colourless solid. Yield = 0.91 g, (49%). δ H (300 MHz, CDCl₃, TMS); 8.28–8.08 (m, 6H, Ar-H), 7.73–7.60 (m, 12H, Ar-H), 7.35 (m, 2H, Ar-H), 7.19 (m, 2H, Ar-H), 7.03 (m, 2H, Ar-H), 5.18 (m, 2H, -C^{*}H(CH₃)-), 4.07 (t, 2H, -CH₂O-, ³J = 6.3 Hz), 2.65 (t, 2H, -CH₂OCO-, ³J = 7.4 Hz), 1.96–1.29 (m, 32H, aliphatic-H), 0.88 (two overlapping triplets, 6H, -CH₂-CH₃). ν /cm⁻¹ (KBr); 2932, 2859 (C-H str.), 1761, 1732, 1717 (C=O str.), 1605 (C-C str.), 831 (1,4-disub. C-H out-of-plane deform.). *m/z*; 944 (M⁺), 472. HPLC purity; Normal phase: 100%, Reverse Phase: 99.4%.

3. RESULTS AND DISCUSSION

Effect of Connecting Two Mesogens

A propyl (*n* = 3) homologue (**3B1M7**) of the monomeric series just showed the SmA phase, however, the corresponding twin compound (**I**) [6] showed broad temperature ranges (ca. 20°C) of antiferroelectric and ferroelectric phases as shown in Figure 2. This is the first example that clearly demonstrates the significant efficacy of connecting two identical mesogenic groups in stabilising a ferroelectric ordering. Furthermore, the absence of head-tail discrimination for this compound presents first unequivocal evidence that the asymmetrical head-tail structure is not essential in generating the ferroelectric structure.

It should be emphasized that the location of the chiral moieties in the over-all molecular structure as well as the structures of chiral centres themselves is a key concept in the molecular design. As described earlier, the twin compound possessing two chiral centres at both peripheral ends of the molecular structure (**I**, Fig. 3) [6] showed a stable ferroelectric phase that is always produced in a highly chiral system.

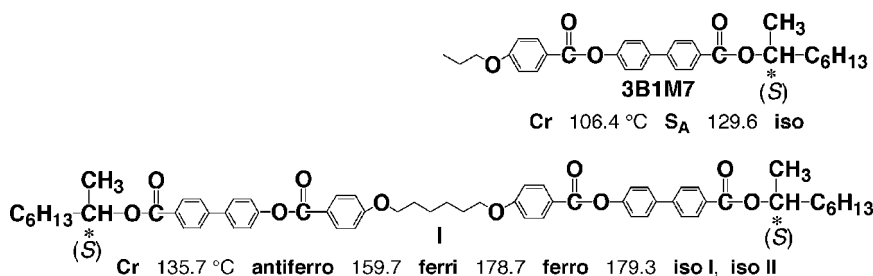


FIGURE 2 Chiral twins and the phase transition behaviour.

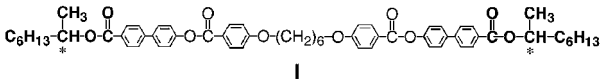
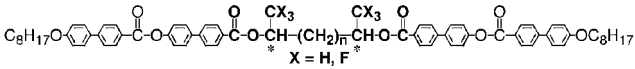
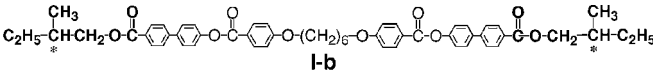
	Phase
 <p style="text-align: center;">I</p>	(Ferro), Ferri, Antiferro
 <p style="text-align: center;">I-a</p>	Ferro, Antiferro
 <p style="text-align: center;">I-b</p>	N*

FIGURE 3 Effect of structure and location of chiral moieties.

However, the related compounds having chiral moieties at the inner part of the molecular structure (**I-a**, Fig. 3) [7] did not show the ferrielectric phase but showed a ferro- or antiferroelectric phase. Even if the chiral moieties locate at the peripheral ends, a different structure lead to the appearance of just a chiral nematic phase (**I-b**, Fig. 3) [8].

Structural Modification

The structure of Compound **I** was then systematically modified in such a way that the number and the location of phenyl rings are varied, thus, analogous non-symmetric chiral twins were prepared according to the novel preparative strategy [9], where two identical chiral moieties were connected by the non-symmetric central group. This molecular design allows us to investigate the effect of introducing a non-symmetric structure without decreasing the number of chiral moieties, as well as without changing the location of the chiral moieties. The effect of the degree of the non-symmetric character was investigated for compounds **II**, **III** and **IV** (see Fig. 4), and the properties were compared with the analogous symmetric twin compound **I**.

Phase transition temperatures obtained for compounds **I**, **II**, **III** and **IV** are listed in Table 1 and are also schematically compared in Figure 5. All of the compounds studied here exhibited ferro-, ferri- and antiferroelectric phases. The symmetric twin **I** showed a broader ferrielectric phase than the other non-symmetric chiral twins. Non-symmetric twin **II** showed two anomalous phases, i.e., *unidentified isotropic* and *mosaic* phases, between the ferroelectric and isotropic liquid phase [9]. The unidentified isotropic phase appeared at a lower

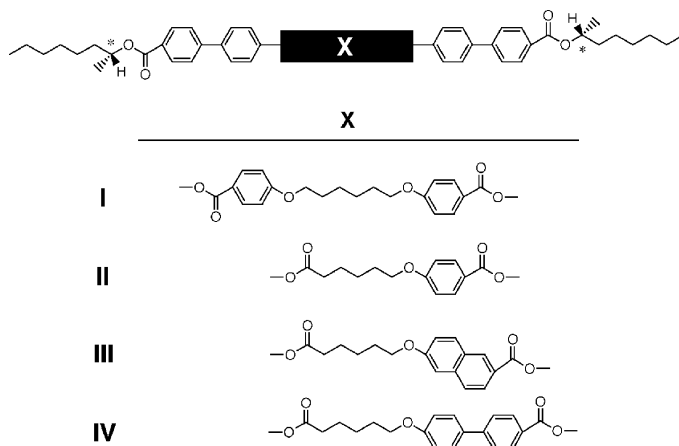


FIGURE 4 Structures of symmetric (**I**) and non-symmetric (**II**, **III**, and **IV**) chiral twin compounds.

temperature region than the mosaic phase. The unidentified isotropic phase looked isotropic under the polarized light microscopy. It should be noted that the unidentified isotropic phase was quite viscous under the shearing of the samples which had been placed between two glass plates. Figure 6 shows the textural change at the ferroelectric-unidentified isotropic phase transition for the pseudo-homeotropically aligned sample of **II** observed using a slightly de-crossed polarized

TABLE 1 Phase Transition Temperatures ($^{\circ}\text{C}$) and Transition Enthalpies (kJ/mol^{-1}) (in *italics*)

	m.p. ^a	anti-ferro	ferri	ferro	SmA	u.i. ^b	mo-saic	iso
I	137.3 <i>55.04</i>	• 159.7 <i>0.48</i>	• 178.1 <i>—^c</i>	•	—	—	— 178.7 <i>2.57^c</i>	• ^d
II	64.1 <i>32.91</i>	• 144.5 <i>0.08</i>	• 146.6 <i>0.07</i>	•	— 148.7 <i>0.66</i>	• 150.7 <i>0.12</i>	• 151.2 <i>7.31</i>	• ^d
III	87.8 <i>36.91</i>	• 156.5 <i>—^e</i>	• 161.4 <i>—^e</i>	• 171.3 <i>0.26</i>	•	—	— 188.9 <i>8.71</i>	• ^d
IV	88.3 <i>28.25</i>	• 205.2 <i>—^e</i>	• 209.6 <i>—^e</i>	• 228.3 <i>0.29</i>	•	—	— 241.6 <i>9.86</i>	• ^d

^aMelting point. ^bUnidentified isotropic phase. ^cPeaks corresponding to the ferri-ferro and ferro-iso transitions were not separated clearly, therefore, only the total enthalpy values for the two transitions were measured. ^dCompound **I** showed a broad diffuse DSC peak of 2.83 kJ/mol in the isotropic phase, however, the other twins did not show such a broad DSC peak. ^eClear DSC peaks were not obtained for these transitions.

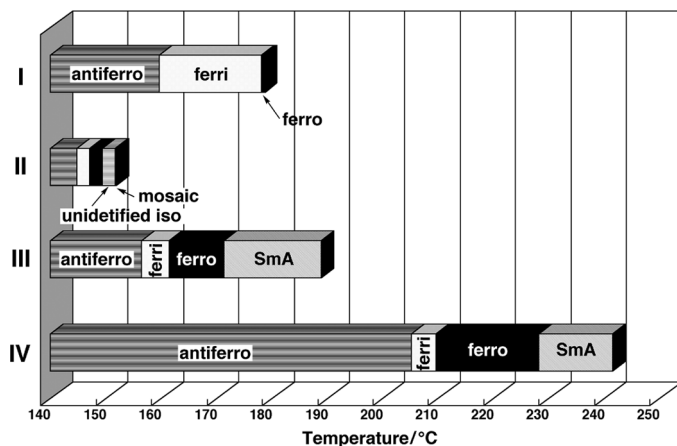


FIGURE 5 Transition temperatures of chiral twin compounds.

light microscope. Round shaped domains of the unidentified isotropic phase appeared in the pseudo-homeotropic texture of the ferroelectric phase. On further heating, both homogeneously and pseudo-homeotropically aligned sample of compound **II** showed a mosaic texture (see Fig. 7), just before the clearing temperature.

Non-symmetric twin compounds, **III** and **IV**, showed the smectic A phase, whereas symmetric twin **I** and non-symmetric twin **II** did not exhibit the smectic A phase. The phase transition behavior observed for **III** and **IV**, i.e., existence of the stable SmA phase and a phase sequence of “ferro-ferri-antiferro” with rather a narrow temperature

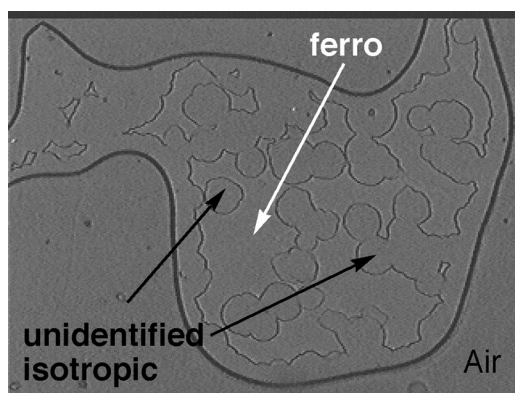


FIGURE 6 Textural change between the pseudo-homeotropic texture of the ferroelectric phase and the unidentified isotropic phase of **II**.

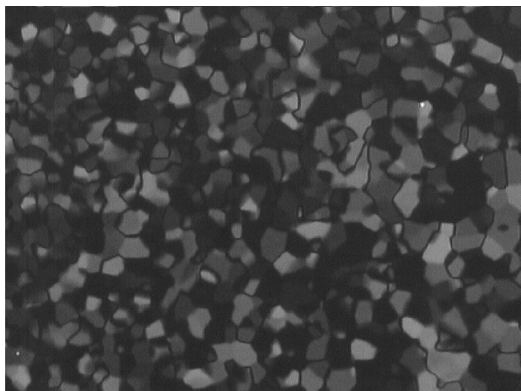


FIGURE 7 Texture of the mosaic phase of **II**.

range of the ferrielectric phase, is quite similar to that obtained for the analogous chiral monomeric liquid crystals [10]. The textures obtained for the ferro-, ferri- and antiferroelectric phases are also quite similar to those obtained for the analogous monomer, where the ferro- and antiferroelectric phases exhibited iridescent textures (see Figs. 8 (a) and (c)), whereas the ferrielectric phase showed a typical white moving texture as shown in Figure 8 (b). These results indicate that the introduction of high degree of non-symmetric character into the twin molecular configuration promotes the monomeric character in the liquid crystal properties.

Differential Scanning Calorimetry Studies

Differential scanning calorimetry (DSC) thermograms for **I**, **II**, **III** and **IV** obtained in the heating process are compared in Figure 9.

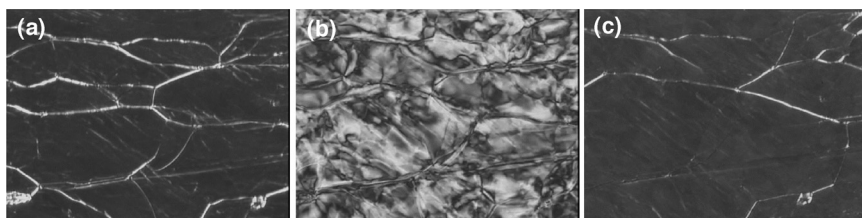


FIGURE 8 Textures obtained for the pseudo-homeotropically aligned sample of non-symmetric chiral twin **IV**: (a) ferro (214°C), (b) ferri (209°C), and (c) anti (165°C).

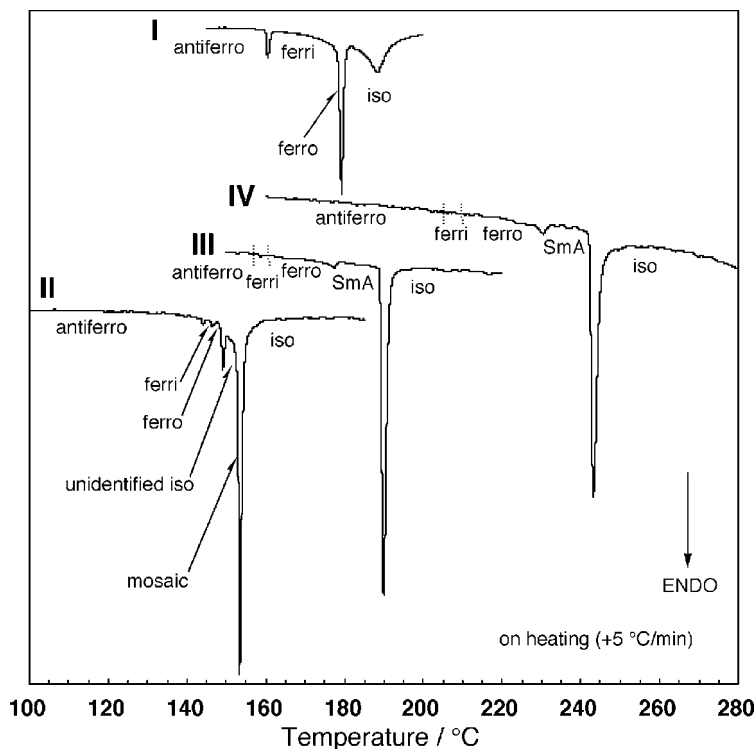


FIGURE 9 DSC Thermograms obtained for the chiral twins.

Symmetric chiral twin I showed a diffuse DSC peak of 2.83 kJ/mol in the isotropic phase [6], whereas the other non-symmetric twins did not show such a bizarre DSC peak. Symmetric twin I showed a clear sharp peak corresponding to the antiferro-ferri transition. However, non-symmetric twins, III and IV, did not show clear peaks corresponding to the transitions between ferro-, ferri-, and antiferroelectric phases, but only showed a small peak corresponding to the SmA-ferroelectric phase transition. The DSC profiles obtained for III and IV are quite similar to those obtained for the analogous monomers, which again supports that high degree of the non-symmetric structure stabilizes the monomeric character. Compound II showed a quite different DSC pattern from the other non-symmetric twins [9]. Small but clear peaks were obtained for the antiferro-ferri and ferri-ferro transitions, and at the clearing point, a large sharp peak was observed.

X-Ray Diffraction Studies

Symmetric chiral twin **I** showed first and second order sharp peaks in the small angle region corresponding to the smectic layer spacing of the ferrielectric and antiferroelectric phases [6b,c]. The appearance of the second order peak indicates the formation of a relatively well-defined smectic layer structure which is considered to be important for generating anticlinic structures in ferrielectric and antiferroelectric phases. In the wide angle region, only diffuse scattering was observed, indicating that there is no positional order within the layers, thus the smectic phases obtained were found to be sub-phases of the smectic C phase. Figure 10 shows the wide angle X-ray diffraction patterns obtained in the antiferro, unidentified isotropic, mosaic and isotropic liquid phases of the non-symmetric chiral twin **II**. In the antiferroelectric phase, a sharp peak corresponding to the smectic layer spacing was observed at the small angle region, however, the second order peak was weaker than symmetric twin **I**, suggesting that **II** possesses less clear smectic layer periodicity than **I**. Only diffuse scattering was observed at the wide angle region, indicating that there is no positional order within the layered structure. Similar X-ray scattering profiles were also obtained for the ferrielectric and ferroelectric phases. Interestingly, even in the unidentified isotropic or mosaic phase, a clear peak was observed in the small angle scattering region, even though the peak intensities were smaller than those obtained for the smectic phases, indicating that the layered structures are more or less formed in the unidentified isotropic and mosaic phases.

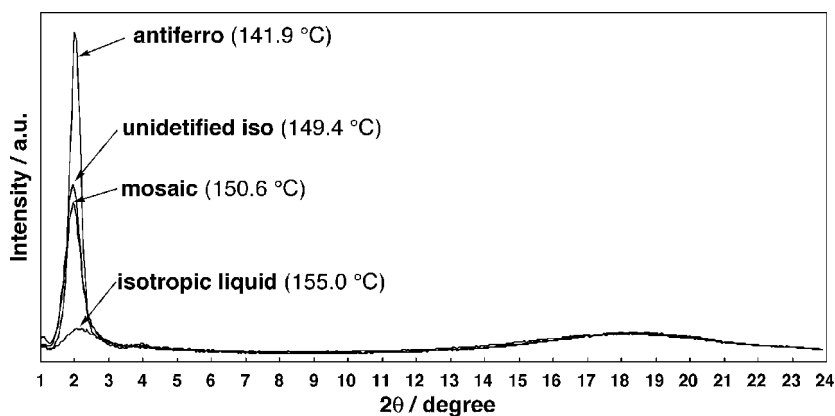


FIGURE 10 X-ray diffraction patterns obtained for non-symmetric chiral twin **II**.

Appearance of the TGB Phase

Symmetric chiral twin **I** showed no SmA phase but only showed tilted smectic phases. Remarkably, however, the 1:1 mixture of (*S, S*) and (*R, R*) isomers exhibited a nematic phase above the smectic C phase. Figure 11 shows the DSC thermograms for symmetric twin **I** and the 1:1 mixture of isomers [6]. The 1:1 mixture showed a sharp peak at nearly same temperature as the broad diffuse peak in the liquid phase for **I**, which corresponds to a nematic to liquid transition. This result suggests that the effect of molecular chirality in symmetric twin **I** considerably depresses the stability of the nematic phase. With a reduction of the optical purity of symmetric twin **I**, no indication of the appearance of the TGB phase was observed.

However, the unidentified isotropic and mosaic phases changed into the TGB phase with a *reduction* in the optical purity of non-symmetric twin **II**, and eventually, the smectic A was obtained for the 1:1 mixture of the (*S, S*)- and (*R, R*)-isomers as shown in Figure 12. These results indicate that unidentified isotropic and mosaic phases possess more strongly twisted molecular assemblies than the TGB structure. Thus, the unidentified isotropic and mosaic phases are considered to have a smectic blue phase like molecular ordering.

Non-symmetric chiral twins **III** and **IV** showed a broad temperature range of the SmA phase, which has been considered not to be suitable for the generation of the TGB phase [1]. Non-symmetric chiral twins **III** and **IV** have more than three aromatic rings at one of the mesogenic parts of each twin molecular configuration, which is expected to produce a stronger ability of the smectic layer formation. Since the TGB is produced as a result of competition between the stabilization of the smectic layered structure and the desire for the

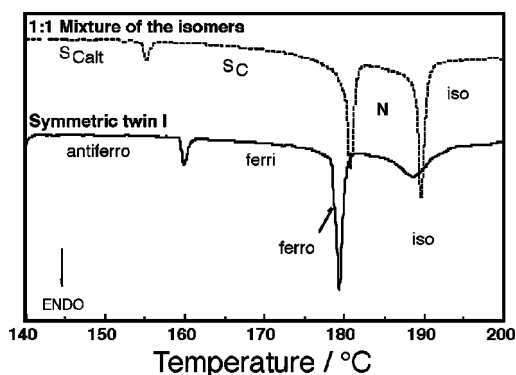


FIGURE 11 DSC thermograms for **I** and the 1:1 mixture of the isomers.

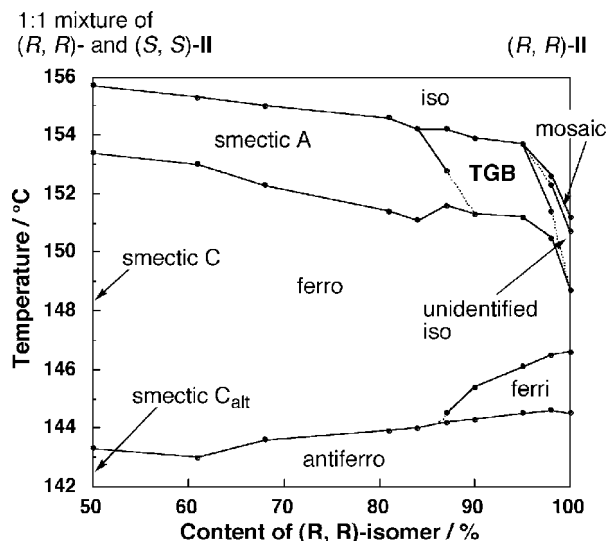


FIGURE 12 Phase diagram between (R, R)-II and the 1:1 mixture of (R, R) and (S, S)-isomers.

molecules to form a helical structure as in the cholesteric phase, the produced smectic structures for **III** and **IV** may be too strong to produce the TGB structure. Non-symmetric twin **II**, however, possesses less aromatic rings than **III** or **IV**, so that the weak layered structure is considered to be produced, which is preferred to the emergence of the TGB and the smectic blue phases.

Molecular Arrangement in the Smectic Phase

The molecular arrangement in the smectic phase is investigated by comparing the observed smectic layer spacing in the SmA phase with the calculated molecular length of each twin. The smectic layer spacings for non-symmetric chiral twins **III** and **IV** in the SmA phase were found to be 47.4 Å and 49.1 Å, respectively. Optically pure **II** itself did not show the SmA phase, but with a reduction in the optical purity, the SmA phase appeared of which the layer spacing was found to be 49.7 Å. Symmetric chiral twin **I** did not show the SmA even if the optical purity is reduced so that the layer spacing obtained in the tilted smectic phase was corrected using the optical tilt angle. Although it has been reported that the optical tilt is different from the steric tilt [11,12], it could provide us a rough measure for the expected SmA layer spacing of **I**. Layer spacing and molecular length are summarized in Figure 13. These results suggest that all of the twin compounds

Compound	Central Structure (X)	Layer Spacing ^a	Molecular Length ^b
I		60.2 Å ^c	57.5 Å
II		49.7 Å	51.0 Å
III		47.4 Å	54.0 Å
IV		49.1 Å	55.4 Å

--

a: Based on the X-ray diffraction measurement in the SmA phase.
 b: Calculated by MM2.
 c: Estimated by the layer spacing in the tilted phase and the optical tilt angle.

FIGURE 13 Comparison between the smectic layer spacing and the molecular structure for chiral twins.

basically exhibit a monolayered smectic structure, not a intercalated structure. Interestingly, however, non-symmetric twins **III** and **IV** apparently showed a shorter smectic layer spacing than expected by the molecular length, indicating that considerable permeation of the tails occurs in the smectic phases of **III** and **IV**.

Anomalous Properties in the Optically Isotropic Phase

In the isotropic phase of dichiral Compounds, **V** and **VI** (Fig. 14), anomalous properties were observed. Compound **V** showed the antiferroelectric and SmQ phases, whereas **VI** showed just an antiferroelectric phase. In the SmQ phase, a typical mosaic texture [3] was observed.

Figure 15 shows a DSC thermogram of Compound **V** together with a small angle X-ray diffraction profile in each phase, obtained in the heating process. Only tiny peaks were observed at the antiferro-SmQ and SmQ-Iso transitions, with enthalpies of 0.53 kJ/mol and 0.34 kJ/mol, respectively. These enthalpy changes are quite small than expected for the considerable difference in the molecular assemblies between the antiferroelectric, SmQ, and isotropic phases.

Characteristic X-ray diffraction profiles were obtained with respect to the phase structures. In the antiferroelectric phase, a ring-shaped scattering was observed as expected for the smectic phase, however,

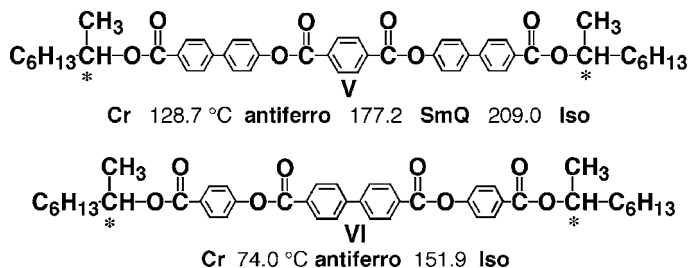


FIGURE 14 Structures of the dichiral compounds.

when the sample was gradually heated into the SmQ phase, the pattern changed drastically. In the SmQ phase, the scattering ring disappeared but lots of spots appeared instead, indicating that the sample was oriented to some extent in the SmQ phase and that the three-dimensional order was generated. Unlike a real crystalline phase, the SmQ phase possesses a liquid-like short range order resulting in a broad scattering in the wide angle region. It should be noted that a certain scattering was obtained even in the isotropic liquid

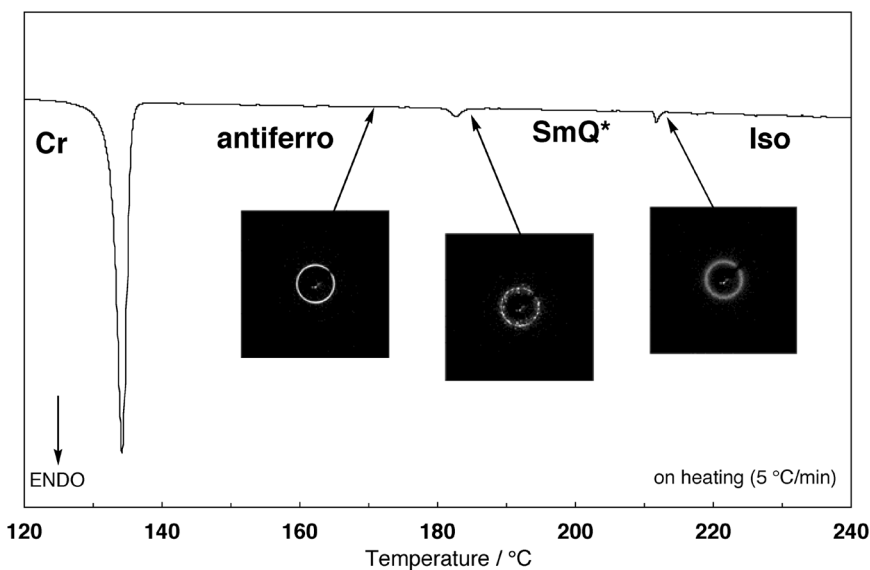


FIGURE 15 A DSC thermogram and X-ray diffraction profiles of Compound V.

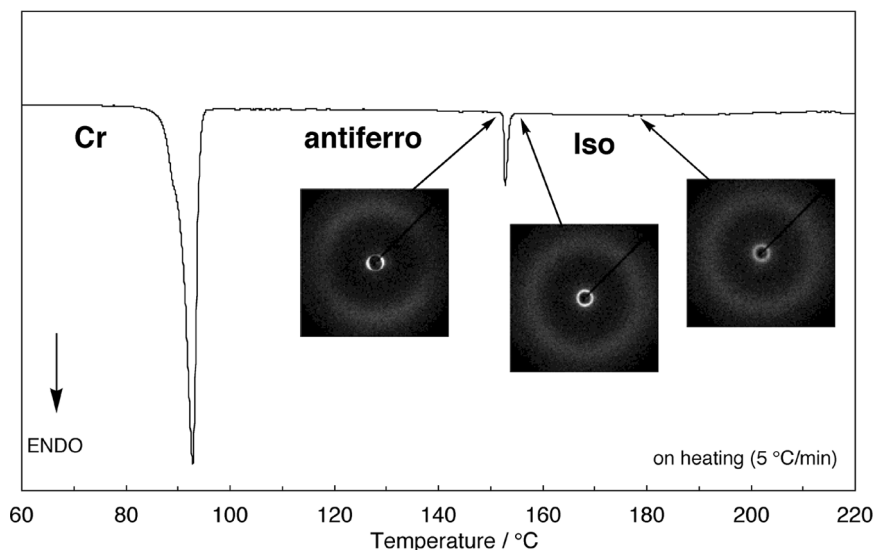


FIGURE 16 A DSC thermogram and X-ray diffraction profiles of Compound **VI**.

phase, suggesting a possible pre-organization of the molecules in the isotropic liquid phase. The obtained significantly small enthalpy change may be attributed to this possible pre-organization of the molecules. Similar anomalous X-ray diffraction in the isotropic phase was also observed for Compound **VI**, as shown in Figure 16. Interestingly, in the isotropic phase of **VI**, the liquid-crystalline phase was induced by applying the electric field. Figure 17 shows the appearance of the liquid crystal phase at ca. 1 degree above the clearing temperature. Without the external electric field, totally dark texture was observed under the crossed polarized light microscope, as usual for the isotropic phase (Fig. 17 (a)). By the application of the electric field, the smectic phase was induced and the fan-shaped texture appeared (Figs. 17 (b) and (c)). This is the first example of the “electric-field induced” isotropic-liquid crystal phase transition. The expected pre-organization of the molecules in the isotropic phase may have close relation to this anomalous phenomenon.

4. CONCLUSION

Systematic structural modifications of the chiral compounds, possessing two chiral centres at both peripheral ends, result in the emergence

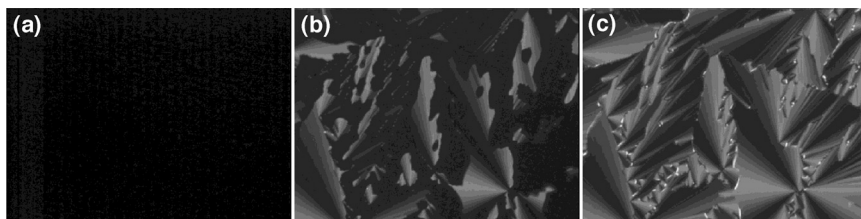


FIGURE 17 Electric field induction of the liquid crystal phase: (a) 0 V/3 μm , (b) 56 V/3 μm , and (c) 68 V/ μm .

	Phase
	SmA
	(Ferro), Ferri, Antiferro
	SmA, Ferro, Ferri, Antiferro
	SmA, Ferro, Ferri, Antiferro
	TGB, Smectic Blue
	New-type SmQ, Sponge
	SmQ

=

FIGURE 18 Dichiral materials and the phase transition behavior.

of novel chiral smectic phases, such as ferri- and antiferroelectric phases, TGB and related phases (i.e., smectic blue and smectic Q phases), and anomalous optically isotropic phases (Fig. 18) [6,9,13].

REFERENCES

- [1] (a) Goodby, J. W., Waugh, M. A., Stein, S. M., Chin, E., Pindak, R., & Patel, J. S. (1989). *Nature*, 337, 449.
 (b) Goodby, J. W., Waugh, M. A., Stein, S. M., Chin, E., Pindak, R., & Patel, J. S. (1989). *J. Am. Chem. Soc.*, 111, 8119.

- [2] (a) Demikhov, E. & Stegmeyer, H. (1991). *Liq. Cryst.*, **10**, 869.
(b) Kitzerow, H.-S. (2001). In: *Chirality in Liquid Crystals*, Kitzerow, H.-S. & Bahr, C. (Eds.), Springer: New York, 346.
- [3] (a) Levelut, A. M., Hallouin, E., Bennemann, D., Heppke, G., & Löttsch, D. (1997). *J. Phys. II*, **7**, 981.
(b) Levelut, A. M., Germain, C., Keller, P., Liebert, L., & Billard, J. (1983). *J. Phys.*, **44**, 623.
(c) Levelut, A. M., Bennemann, D., Heppke, G., & Löttsch, D. (1997). *Mol. Cryst. Liq. Cryst.*, **299**, 433.
(d) Bennemann, D., Heppke, G., Levelut, A. M., & Löttsch, D. (1995). *Mol. Cryst. Liq. Cryst.*, **260**, 351.
- [4] (a) Yoshizawa, A., Umezawa, J., Ise, N., Sato, R., Soeda, Y., Kusumoto, T., Sato, K., Hiyama, T., Takanishi, Y., & Takezoe, H. (1998). *Jpn. J. Appl. Phys.*, **37**, L942.
(b) Kusumoto, T., Sato, K., Katoh, M., Matsutani, H., Yoshizawa, A., Ise, N., Umezawa, J., Takanishi, Y., Takezoe, H., & Hiyama, T. (1999). *Mol. Cryst. Liq. Cryst.*, **330**, 227.
- [5] Takanishi, Y., Takezoe, H., Yoshizawa, A., Kusumoto, T., & Hiyama, T. (2000). *Mol. Cryst. Liq. Cryst.*, **347**, 257.
- [6] (a) Nishiyama, I., Yamamoto, J., Goodby, J. W., & Yokoyama, H. (2001). *J. Mater. Chem.*, **11**, 2690.
(b) Nishiyama, I., Yamamoto, J., Goodby, J. W., & Yokoyama, H. (2002). *Liq. Cryst.*, **29**, 1409
(c) Nishiyama, I., Yamamoto, J., Goodby, J. W., & Yokoyama, H. (2002). *Ferroelectrics.*, **276**, 255.
- [7] (a) Suzuki, Y., Isozaki, T., Kusumoto, T., & Hiyama, T. (1995). *Chem. Lett.*, **24**, 719.
(b) Suzuki, Y., Isozaki, T., Hashimoto, S., Kusumoto, T., Hiyama, T., Takanishi, Y., Takezoe, H., & Fukuda, A. (1996). *J. Mater. Chem.*, **6**, 753.
- [8] Choi, E.-J., Choi, B.-K., Kim, J.-H., & Jin, J.-I. (2000). *Bull. Korean Chem. Soc.*, **21**, 110.
- [9] Nishiyama, I., Yamamoto, J., Goodby, J. W., & Yokoyama, H. (2002). *J. Mater. Chem.*, **12**, 1709.
- [10] Goodby, J. W., Patel, J. S., & Chin, E. (1992). *J. Mater. Chem.*, **2**, 197.
- [11] Goodby, J. W., Chin, E., Leslie, T. M., Geary, J. M., & Patel, J. S. (1986). *J. Am. Chem. Soc.*, **108**, 4729.
- [12] Mills, J. T., Gleeson, H. F., Goodby, J. W., Hird, M., Seed, A., & Styring, P. (1998). *J. Mater. Chem.*, **8**, 2385.
- [13] Nishiyama, I., Yamamoto, J., Goodby, J. W., & Yokoyama, H. (2004). *Chem. Mater.*, **16**, 3212.